ORIGINAL PAPER

Synthesis and Properties of Salicyladehyde Salicyhydrazone Derivatives and Their Europium Complexes

Defen Meng · Fen Liu · Xiaomei Lian · Zehui Yang · Dongcai Guo

Abstract Four novel salicyladehyde salicyhydrazone derivatives and their corresponding europium (Eu^{3+}) complexes were synthesized and characterized. The formulas of the complexes were [EuL^{a-d}(NO$_3$)$_2$](NO$_3$)·H$_2$O. The investigatoin of fluoresence properties of the Eu^{3+} complexes showed that the salicyladehyde salicyhydrazone derivatives were efficient sensitizers for the fluoresence of Eu^{3+} ions. The fluorescence intensity of the complex substituted by methyl (−CH$_3$) was the strongest among all the Eu^{3+} complexes. The exploration of the electrochemical properties of the Eu^{3+} complexes showed that the introduction of electron-donating groups methyl and methoxyl (−CH$_3$ and −OCH$_3$) could increase the oxidation potential and the highest occupied molecular orbital (HOMO) energy level of the Eu^{3+} complex; however, the results of introduction of electron-withdrawing group were just opposite.

Keywords Europium complexes · Salicyhydrazone derivatives · Synthesis · Fluorescence · Electrochemical properties

Introduction

Study of fluorescence enhancement of Eu^{3+} ions in the presence of schiff bases is of special interest, because the Eu^{3+} complexes with schiff bases are frequently used as structural and functional probes in biological systems and have technological applications in lasers, sensors, electroluminescence displays [1–4]. However, the free Eu^{3+} ions have a low absorbance in rather narrow bands, and the direct excitation yields only a weak luminescence. This luminescence can be strengthened if a stable complex is formed with a suitable organic ligand, which can transfer its excitation energy to Eu^{3+} ions.

Salicyladehyde salicyhydrazone containing C=N group possesses strong conjugated system and high intramolecular electron transfer efficiency [5], so the luminescence of Eu^{3+} ions can be enhanced when they are coordinated to the Eu^{3+} ions.

In this paper, salicyladehyde salicyhydrazone derivatives and corresponding complexes were synthesized. The fluorescence properties and the fluorescence quantum yields of the Eu^{3+} complexes were studied. Meanwhile, the relationship between the structure of the ligands and the electrochemical properties of the Eu^{3+} complexes were discussed in detail. The synthetic route for the salicyladehyde salicyhydrazone derivatives is shown in Scheme 1.

D. Meng · F. Liu · X. Lian · D. Guo (✉)
School of Chemistry and Chemical Engineering, Hunan University,
Changsha 410082, China
e-mail: dcguo2001@163.com

Z. Yang
School of Chemical Engineering, Ningbo University of Technology,
Ningbo 315016, China

Experimental

Materials and Methods

Europium nitrate was prepared according to the literature [6]. Aniline and its derivatives were of chemical grade. Methyl salicylate and other reagents were of analytical grade and purchased from commercial suppliers.

^{1}H nuclear magnetic resonance (^{1}H NMR) spectra were recorded in dimethyl sulfoxide (DMSO)-d$_6$/deuterated chloroform (CDCl$_3$) on Brucker spectrophoto-meter (400 MHz) with TMS as an internal standard. Mass spectra (MS) were measured with the MAT95XP Mass Spectrometer. Infrared (IR) spectra (400 cm^{-1}−4,000 cm^{-1}) were obtained in KBr

Scheme 1 The synthetic route for the salicyladehyde salicyhydrazone derivatives
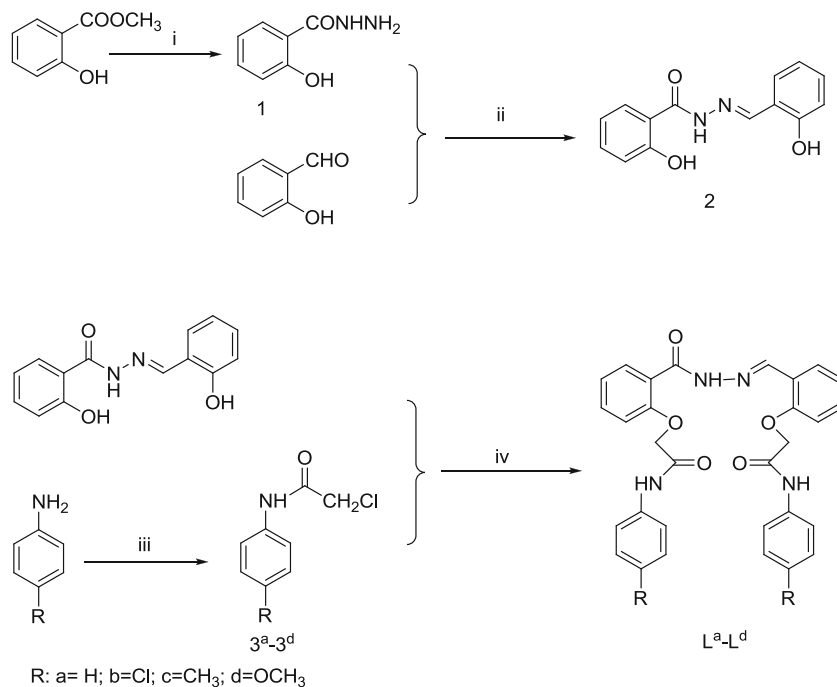
i: NH₂NH₂·H₂O/EtOH/reflux   ii: EtOH/reflux
iii: ClCH₂COCl/CH₃COOH/0 °C   iv: NaOH/KI/DMF/reflux

discs by a PERKIN-ELMER Spectrum One. Ultraviolet-visible (UV-Visible) spectra (190–450 nm) were recorded by LabTech UV-2100 spectrophotometer, with DMSO as solvent and reference. Elemental analysis of the complexes was carried out on a VarioEL 111 (Germany) CHNS analyzer. Melting points of all compounds were determined on an X-4 binocular microscope. Thermal gravimetric analysis was carried out on a NETZSCH STA 409PC thermal gravimetric analyzer. The fluorescence spectra were measured by using powder samples on a HIACHI F-2700 Fluorescence Spectrophotometer at room temperature. Molar conductance was measured by DDS-12A conductivity instrument. The europium ion was determined by ethylenediaminetetraacetic acid (EDTA) titration using xylenol orange as an indicator. Cyclic voltammetry curves were tested using three electrodes including glassy electrode, a platinum electrode and a saturated calomel electrode, with ferrocene as external standard, and nitrite solution was used as the supporting electrolyte and dimethyl sulfoxide as the solvent, the test scanning speed was 100 mV·s^{-1} and the sensitivity was 1 mA.

General Procedure for Synthesis of the Intermediates

Synthesis of Compound 2

The synthesis of salicyladehyde salicyhydrazone was according to the literature [7]. A mixture of methyl salicylate (0.1 mol, 13.81 g), hydrazine hydrate (30 mL 80 %) and absolute alcohol (EtOH) (30 mL) was added to the 150 mL three-neck flask and heated to reflux for 4 h. The excess absolute alcohol was completely removed under reduced pressure. The residue was recrystallized from water to give compound 1. It was used for the next reaction directly without further purification.

The above product (0.02 mol, 3.04 g) and absolute alcohol (30 mL) were heated to boiling with stirring, then salicyladehyde (0.02 mol, 2.12 g) dissolved in 15 mL absolute alcohol was added to it dropwise. The reaction mixture was refluxed for 6 h, cooled to room temperature, and then filtered. The residue was recrystallized from absolute alcohol to get yellow solid.

Salicyladehyde salicyhydrazone (2) Yield: 96 %. ^{1}H NMR (400 MHz, DMSO-d$_6$), δ/ppm: 6.92−7.01 (m, 4H, ArH), 7.32 (d, 1H, ArH), 7.46 (d, 1H, ArH), 7.58 (dd, 1H, ArH), 7.90 (dd, 1H, ArH), 8.69 (s, 1H, NH), 11.20 (s, 1H, CH=N), 11.78 (s, 1H, OH), 12.05 (s, 1H, OH); MS (EI) m/z (%): 264 (M+18, 3), 257 (M+1, 5), 256 (M, 33), 137 (M-119, 36), 121 (M-119-16, 100), 120 (40), 93 (15), 65 (15).

Synthesis of Compound 3

Aniline (0.066 mol, 6.15 g) was dissolved in glacial acetic acid (40 mL) in a 150 mL single-neck flask, and then 2-chloride-acetyl chloride (0.074 mol, 8.36 g) was added to it dropwise under ice bath. The reaction mixture was stirred for 30 min under ice bath and for another 1 h

at room temperature. The resulting mixture was poured into saturated sodium acetate solution (300 mL) and then filtered. The residue was recrystallized from the mixed solution of EtOH and water (V_{EtOH}: V_{water}=1:2) to obtain the compound 3^a. The general synthesis procedures of 3^{b-d} are similar to that of 3^a.

2-chloro-N-phenylacetamide (3^a) A white solid. Yield: 68 %. ^{1}H NMR (400 MHz, DMSOd$_6$), δ/ppm: 10.29 (s, 1H, NH), 7.77−7.47 (m, 2H, ArH), 7.40−7.22 (m, 2H, ArH), 7.18 −6.95 (m, 1H, ArH), 4.25 (s, 2H, CH$_2$); MS (EI) m/z (%): 172 (M+3, 3), 171 (M+2, 25), 169 (M, 80), 121 (3), 120 (40), 106 (7), 94 (10), 93 (100), 77 (22), 65 (28).

2-chloro-N-(4-chlorophenyl)acetamide (3^b) A white solid. Yield: 94 %. ^{1}H NMR (400 MHz, DMSO-d$_6$), δ/ppm: 7.67− 7.57 (m, 2H, ArH), 7.46−7.34 (m, 2H, ArH), 4.26 (s, 2H, CH$_2$); MS (EI) m/z (%): 207 (M+3, 5),205 (M+1, 33), 203 (M−1, 52), 156 (4), 154 (13), 129 (32),127 (100), 126 (15), 111 (5), 99 (14), 77 (5), 63 (7).

2-chloro-N-p-tolyacetamide (3^c) A faint solid. Yield: 78 %. ^{1}H NMR (400 MHz, DMSO-d$_6$), δ/ppm: 10.21 (s, 1H, NH), 7.42−7.46 (m, 2H, ArH), 7.16−7.18 (m, 2H, ArH), 4.22 (s, 2H, CH$_2$), 2.21 (s, 3H, CH$_3$); MS (EI) m/z (%): 186 (M+3, 3), 185 (M+2, 25), 183 (M, 75), 148 (4), 134 (27), 107 (100), 106 (76), 91 (16),77 (26), 51 (10).

2-chloro-N-(4-methoxyphenyl)acetamide (3^d) A faint purple solid. Yield: 53 %. ^{1}H NMR (400 MHz, DMSO-d$_6$), δ/ppm: 10.18 (s, 1H, NH), 7.54−7.48 (m, 2H, ArH), 6.95−6.87 (m, 2H, ArH), 4.22 (s, 2H, CH$_2$), 3.73 (s, 3H, CH$_3$); MS (EI) m/z (%): 202 (M+3, 3), 201 (M+2, 32), 199 (M, 100), 124 (29), 123 (72), 108 (72), 95 (13), 80 (6).

Synthesis of the Salicyladehyde Salicyhydrazone Derivatives L^{a-d}

A mixture of compound 2 (3 mmol, 0.77 g) and NaOH (6 mmol, 0.24 g) was dissolved in 40 mL dimethylformamide (DMF) and heated to 80 °C with stirring for 1.5 h in a 150 mL three-neck flask. The mixture of compound 3^a (6.6 mmol, 1.12 g) and KI (3.3 mmol, 0.55 g) dissolved in 30 mL DMF was added into the flask slowly. The resulting mixture was stirred

for 20 h at 80 °C, and then the solvent DMF was completely removed under reduced pressure. The residue was poured into 150 mL distilled water and stirred for 30 min. The precipitate was filtered, washed with water and recrystalled from the mixed solution of absolute alcohol and chloroform (CHCl$_3$) (V_{EtOH}:V_{CHCl3}= 1:3) to give L^a. The general synthesis procedures of L^{b-d} are similar to that of L^a.

(E) - 2 - (2 - ((2 - (2 - (2 - o x o - 2-(phenylamino)ethoxy)benzoyl)hydrazono)methyl)phenoxy)-N-phenylacetamide (L^a) A earthy yellow power. Yield: 85 %. M.p.: 218 °C. ^{1}H NMR (400 MHz, DMSO-d$_6$), δ/ppm: 11.21 (s, 1H, CH=N), 8.68 (s, 1H, NH), 7.94−7.87 (m, 4H, ArH), 7.82 (dt, J=12.8, 6.4 Hz, 2H, ArH), 7.70 (t, J= 7.8 Hz, 4H, ArH), 7.53 (s, 2H, NH), 7.33 (ddd, J=16.8, 12.3, 6.2 Hz, 4H, ArH), 7.26−7.10 (m, 4H, ArH), 4.98 (s, 4H, CH$_2$); IR (KBr) v/cm^{-1}: 3416, 3057, 2920, 2857, 1651, 1605, 1550, 1484, 1446, 1239, 1056, 827, 745, 689; MS (EI) m/z (%): 523 (M+1, 2), 522 (M, 10), 389 (M-77-15-28-13, 10), 270 (11), 254 (17), 226 (20), 177 (8), 134 (22), 121 (100), 106 (50), 93 (45), 77 (18); Anal. Calcd. for C$_{30}$H$_{26}$N$_4$O$_5$: C, 68.95; H, 5.02; N, 10.72; O, 15.31. Found: C, 68.92; H, 5.06; N, 10.71.

(E) - N - (4 - c h l o r o p h e n y l) 2 - (2 - ((2 - (2 - (4 - c h l o r o p h e n y l a m i n o) - 2 - oxoethoxy)benzoyl)hydrazono)methyl)phenoxy)acetamide (L^b) A terreous power. Yield: 89 %. M.p.: 235 °C. ^{1}H NMR (400 MHz, DMSO-d$_6$), δ/ppm: 11.34 (s, 1H, CH=N), 8.97 (s, 1H, NH), 8.77 (s, 1H, ArH), 8.08 (dd, J=29.2, 8.3 Hz, 5H, ArH), 7.64−7.53 (m, 8H, ArH), 7.43 (s, 2H, NH), 7.02 (dd, J=18.9, 7.9 Hz, 2H, ArH), 4.32 (s, 4H, CH$_2$); IR (KBr) v/cm^{-1}: 3402, 3042, 2918, 2856, 1658, 1604 ,1575, 1494, 1453, 1246,1049, 820; MS (EI) m/z (%): 608 (M+18, 1), 591 (M+1, 2), 590 (M, 8), 464 (M-35-76-15, 10), 423 (15), 304 (21), 288 (44), 260 (24), 211 (10), 177 (8), 134 (24), 121 (100), 106 (48), 91 (36), 77 (18); Anal. Calcd. for C$_{30}$H$_{24}$Cl$_2$N$_4$O$_5$: C, 60.92; H, 4.09; Cl, 11.99; N, 9.47; O, 13.53. Found: C, 60.95; H, 4.11; Cl, 11.97; N, 9.44.

(E) - 2 - (2 - ((2 - (2 - (2 - o x o - 2 - (p - tolylamino)ethoxy)benzoyl)hydrazono)methyl)phenoxy)-N-p-tolyacetamide (L^c) A brown power. Yield: 84 %. M.p.: 239 °C. ^{1}H NMR (400 MHz, CDCl$_3$), δ/ppm: 11.46 (s, 1H,

Table 1 The elemental analysis and molar conductance data of the europium complexes

Complex	Found (calculated) (%)				Λ_m
	C	H	N	Eu	(S·cm^2·mol^{-1})
[EuL^a(NO$_3$)$_2$](NO$_3$)·H$_2$O	41.24 (41.01)	3.28 (3.21)	11.25 (11.16)	17.21 (17.30)	105
[EuL^b(NO$_3$)$_2$](NO$_3$)·H$_2$O	37.89 (38.03)	2.76 (2.77)	10.25 (10.35)	16.32 (16.04)	111
[EuL^c(NO$_3$)$_2$](NO$_3$)·H$_2$O	42.43 (42.39)	3.71 (3.56)	10.56 (10.81)	16.45 (16.76)	132
[EuL^d(NO$_3$)$_2$](NO$_3$)·H$_2$O	40.76 (40.95)	3.36 (3.44)	10.21 (10.45)	16.42 (16.19)	126

CH=N), 8.84 (s, 1H, NH), 7.49 (dd, J=10.0, 3.7 Hz, 4H, ArH), 7.42 (m, 2H, NH), 7.34 (dd, J=15.0, 8.0 Hz, 4H, ArH), 7.13 (dd, J=11.6, 9.1 Hz, 4H, ArH), 7.00 (dd, J=14.3, 8.4 Hz, 2H, ArH), 6.85 (dd, J=8.6, 3.3 Hz, 1H, ArH), 6.78 (d, J= 7.9 Hz, 1H, ArH), 4.64 (s, 4H, CH_2), 3.49 (s, 6H, CH_3); IR (KBr) v/cm^{-1}: 3421, 3056, 2913, 2866, 1647, 1602, 1541, 1485, 1453, 1246, 1056 816; MS (EI) m/z (%): 568 (M+18, 1), 551 (M+1, 2), 550 (M, 6), 444 (M-15-76-15, 3), 403 (18), 284 (25), 268 (43), 240 (27), 227 (2), 209 (7), 191 (3), 177 (6), 134 (26), 121 (100), 106 (42), 91 (24), 77 (19); Anal. Calcd. for $C_{32}H_{30}N_4O_5$: C, 69.80; H, 5.49; N, 10.18; O, 14.53. Found: C, 69.84; H, 5.51; N, 10.16.

(E)-N-(4-methoxyphenyl)2-(2-((2-(2-(2-(4−methoxyphenylamino)-2-oxoethoxy)benzoyl)hydrazono)methyl)phenoxy)acetamide (L^d) A yellow power. Yield: 56 %. M.p.: 252 °C. ^1H NMR (400 MHz, DMSO-d_6), δ/ppm: 11.34 (s, 1H, CH=N), 8.38 (s, 1H, NH), 7.72 (d, J=8.3 Hz, 2H, ArH), 7.43 (dd, J=15.9, 7.8 Hz, 6H, ArH), 7.34 (dd, J=15.4, 8.4 Hz, 2H, ArH), 724 (s, 2H, NH), 7.17−7.08 (m, 1H, ArH), 7.04–6.95 (m, 1H, ArH), 6.85 (dt, J=15.9, 10.5 Hz, 2H, ArH), 6.78 (d, J=7.9 Hz, 2H, ArH), 4.63 (s, 4H, CH_2), 3.72 (s, 6H, CH_3); IR (KBr) v/cm^{-1}: 3394, 3063, 2911, 2834, 1659, 1602, 1582, 1509, 1454, 1240, 1056, 827; MS (EI) m/z (%): 582 (M, 12), 419 (M-15-16-76-15, 8), 300 (12), 284 (41), 256 (22), 207 (12), 177 (6), 134 (26), 121 (100), 106 (48), 91 (42), 77 (20); Anal. Calcd. for $C_{32}H_{30}N_4O_7$: C, 65.97; H, 5.19; N, 9.62; O, 19.22. Found: C, 65.94; H, 5.22; N, 9.67.

Synthesis of the Eu^{3+} Complexes

A mixture of compound L^a (0.5 mmol, 0.26 g) and $CHCl_3$ (30 mL) was heated to reflux at 80 °C in a 100 mL three-neck flask, and then the europium nitrate dissolved in absolute alcohol (5 mL) was added to it to produce precipitate. Then, the mixture was refluxed for 4 h. The solid product was filtered, washed with $CHCl_3$ several times, and dried under a vacuum to give complex with ligand L^a. The general synthesis procedures of other complexes with ligands $L^{b−d}$ are similar to that of complex with ligand L^a.

Fig. 1 The UV-Visible spectra of $[EuL^a(NO_3)_2](NO_3)\cdot H_2O$ (a) and L^a (b)
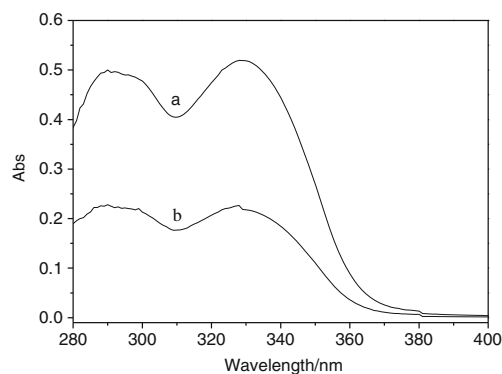
Results and Discussion

Elemental Analysis and Solubility of the Eu^{3+} Complexes

The data of the elemental contents (C, H, N and Eu) of all the Eu^{3+}complexes are listed in Table 1, which are, within the experimental error, in good agreement with the values calculated, indicating that the composition of the complexes is consistent to formulas of $[EuL^{a−d}(NO_3)_2](NO_3)\cdot H_2O$. Ligands $L^{a−d}$ are easily dissolved in DMSO, DMF, and partially dissolved in $CHCl_3$, but hardly dissolved in ethyl ether and benzene, while the Eu^{3+} complexes are only dissolved in DMSO and DMF. The molar conductance values of the complexes in acetone solution are in the range of 105–132 S·cm^2·mol^{-1}, which indicats that the Eu^{3+} complexes are 1:1 electrolytes [8]. The elemental contents (C, H, N and Eu) of the Eu^{3+} complexes are quite close to those calculated from molecular formula proposed, which indicates the correctness of molecular composition proposed.

UV-Visible Analysis

The UV-Visible absorption spectra of the Eu^{3+} complexes and corresponding ligands were recorded in DMSO solution, and

Table 2 The UV data of the europium complexes and corresponding ligands

Complex	λ_{max}/nm	Ligand	λ_{max}/nm
$[EuL^a(NO_3)_2](NO_3)\cdot H_2O$	291, 328	L^a	290, 326
$[EuL^b(NO_3)_2](NO_3)\cdot H_2O$	289, 324	L^b	287, 321
$[EuL^c(NO_3)_2](NO_3)\cdot H_2O$	288, 321	L^c	287, 318
$[EuL^d(NO_3)_2](NO_3)\cdot H_2O$	288, 318	L^d	286, 316

Fig. 2 The UV-Visible spectra of $[EuL^c(NO_3)_2](NO_3)\cdot H_2O$ (a) and L^c (b)

Table 3 The IR data of the europium complexes and corresponding ligands

Compound	ν_{Ar-H}	$\nu_{Ar-C=C}$	$\nu_{C=N}$	$\nu_{N-C=O}$	ν_{Ar-O-C}	$\nu_{NO_3}^{-1}$
L^a	3,057	1,550, 1,484	1,605	1,651	1,239	
$[EuL^a(NO_3)_2](NO_3)\cdot H_2O$	3,063	1,550, 1,498	1,618	1,675	1,252	1,474, 1,383, 1,039, 835
L^b	3,042	1,575, 1,494	1,604	1,658	1,246	
$[EuL^b(NO_3)_2](NO_3)\cdot H_2O$	3,055	1,572, 1,510	1,609	1,669	1,248	1,482, 1,379, 1,034, 835
L^c	3,056	1,541, 1,485	1,602	1,647	1,246	
$[EuL^c(NO_3)_2](NO_3)\cdot H_2O$	3,057	1,542, 1,489	1,612	1,662	1,249	1,476, 1,383, 1,032, 817
L^d	3,063	1,582, 1,509	1,602	1,659	1,240	
$[EuL^d(NO_3)_2](NO_3)\cdot H_2O$	3,064	1,550, 1,492	1,618	1,687	1,260	1,482, 1,384, 1,041, 836

the data are listed in Table 2. Since UV-Visible spectra of all complexes are similar, only the UV-Visible spectra of $[EuL^a(NO_3)_2](NO_3)\cdot H_2O$ and $[EuL^c(NO_3)_2](NO_3)\cdot H_2O$ as well as their corresponding ligands L^a and L^c are selected, as shown in Figs. 1 and 2, respectively.

As shown in Figs. 1 and 2, the UV-Visible spectral shapes of the complexes $[EuL^a(NO_3)_2](NO_3)\cdot H_2O$ and $[EuL^c(NO_3)_2](NO_3)\cdot H_2O$ are similar to that of the free ligands L^a and L^c, which suggests that the coordination of Eu^{3+} ions does not have a significant influence on the $\pi\rightarrow\pi*$ and $n\rightarrow\pi*$ state energy, and also reveals that the absorption of the Eu^{3+} complexes is mainly attributed to the ligands. It can be seen from Table 2 that the UV-Visible absorption spectra of $[EuL^a(NO_3)_2](NO_3)\cdot H_2O$, $[EuL^b(NO_3)_2](NO_3)\cdot H_2O$, $[EuL^c(NO_3)_2](NO_3)\cdot H_2O$ and $[EuL^d(NO_3)_2](NO_3)\cdot H_2O$ both exhibit two peaks at 291 nm and 328 nm, 289 nm and 324 nm, 288 nm and 321 nm, 288 nm and 318 nm, due to intraligand $\pi\rightarrow\pi*$ and $n\rightarrow\pi*$ transitions, respectively, which are red shifted compared to the broad absorption peaks at 290 nm and 326 nm, 287 nm and 321 nm, 287 nm and 318 nm, 286 nm and 316 nm for the free ligands L^a, L^b, L^c and L^d, respectively. This indicates that the conjugative effect increases due to the perturbation induced by the Eu^{3+} ions when the nitrogen atom of C=N group and the oxygen atom of C=O

group of L^a and L^c are coordinated successfully to the central Eu^{3+} ions [9].

Infrared Spectra Analysis

The IR data of the ligands and their Eu^{3+} complexes are listed in Table 3. Since the IR spectra of all the complexes are similar, only the IR spectra of $[EuL^a(NO_3)_2](NO_3)\cdot H_2O$ and $[EuL^c(NO_3)_2](NO_3)\cdot H_2O$ as well as their corresponding ligands are selected (Figs. 3 and 4, respectively).

As shown in Figs. 3 and 4, the free ligands L^a and L^c exhibit absorption bands at 1605 cm^{-1} and 1602 cm^{-1}, respectively, which are assigned to the ν (C=N) stretching vibration, while the absorption bands of their corresponding Eu^{3+} complexes shift by about 13 cm^{-1} and 10 cm^{-1} to a higher frequency, implying that the nitrogen atom of C=N group coordinates to the Eu^{3+} ions [10]. The bands at 1651 cm^{-1} and 1647 cm^{-1} of L^a and L^c, respectively, are attributed to the ν (N-C=O) group stretching modes. In the Eu^{3+} complexes, the ν (N-C=O) peaks shifted upfield by 24 cm^{-1} and 15 cm^{-1} indicate that the oxygen atom of N-C=O group takes part in coordination to the Eu^{3+} ions. The absorption bands of L^a and L^d appeared at 1240 cm^{-1} and 1050 cm^{-1}, respectively,
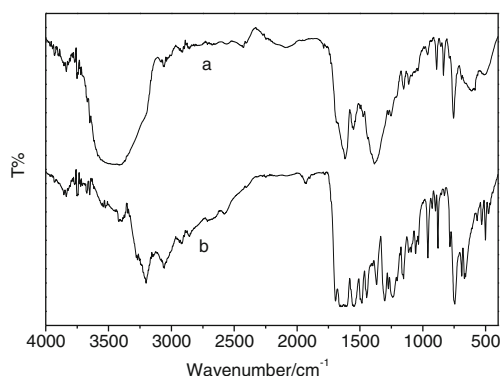
Fig. 3 The IR spectra of $[EuL^a(NO_3)_2](NO_3)\cdot H_2O$ (**a**) and L^a (**b**)
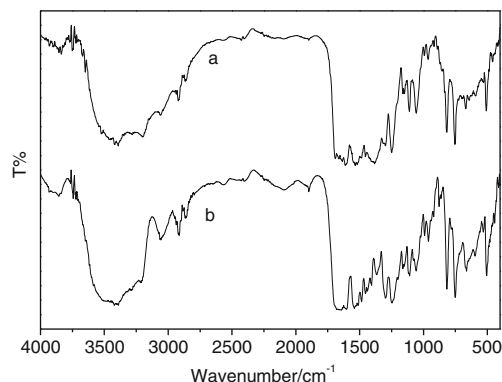
Fig. 4 The IR spectra of $[EuL^c(NO_3)_2](NO_3)\cdot H_2O$ (**a**) and L^c (**b**)

Table 4 The thermogravimetric data of the europium complexes

Complex	H$_2$O (lost) (calcd)(%)	NO$_3$ (lost) (calcd)(%)	Ligand (lost) (calcd)(%)	Metal reside (calcd)(%)
[EuL^a(NO$_3$)$_2$](NO$_3$)·H$_2$O	2.24 (2.05)	21.45 (21.16)	58.13 (59.39)	16.88 (17.40)
[EuL^b(NO$_3$)$_2$](NO$_3$)·H$_2$O	2.02 (1.90)	19.91 (19.64)	60.10 (62.30)	15.86 (16.16)
[EuL^c(NO$_3$)$_2$](NO$_3$)·H$_2$O	2.07 (1.98)	20.72 (20.51)	59.44 (60.64)	16.01 (16.87)
[EuL^d(NO$_3$)$_2$](NO$_3$)·H$_2$O	2.03 (1.92)	20.18 (19.83)	61.70 (62.05)	15.98 (16.20)

attribute to the stretching vibration of the Ar-O-C group, but it does not shift obviously in the Eu^{3+} complexes, indicating that the oxygen atom of Ar-O-C group does not coordinate to the Eu^{3+} ions.

It can be seen from Table 3 that the characteristic frequencies of the coordinating nitrate groups in [EuL^a(NO$_3$)$_2$](NO$_3$)·H$_2$O appeared approximately at 1479 (υ_1), 1369 (υ_4), 1033 (υ_2) and 835 cm^{-1} (υ_3). In addition, the difference between the two strongest absorption bands of the nitrate groups ($|\upsilon_1–\upsilon_4|$) can be defined as $\Delta\upsilon$. It is generally believed that the $\Delta\upsilon$ value is below 200 for the bidentate nitrate moiety, but above 200 for the monodentate nitrate moiety [11]. While, the $\Delta\upsilon$ values of [EuL^a(NO$_3$)$_2$](NO$_3$)·H$_2$O and [EuL^c(NO$_3$)$_2$](NO$_3$)·H$_2$O are about 91 cm^{-1} and 93 cm^{-1}, respectively, which indicate that the nitrate groups coordinate to the Eu^{3+} ions as bidentate ligands. Meanwhile, there are free nitrate groups in the Eu^{3+} complexes, which are consistent with the results of the conductivity experiment, and confirmed in the following thermogravimetric analysis.

Thermal Analysis

To examine the thermal stability and details of thermal decomposition of the Eu^{3+} complexes, the thermogravimetric analysis was carried out and the data are listed in Table 4. Since the four Eu^{3+} complexes present similar thermal behavior, we only give the TG-DSC curve of [EuL^a(NO$_3$)$_2$](NO$_3$)·H$_2$O (Fig. 5) as example for illustration.
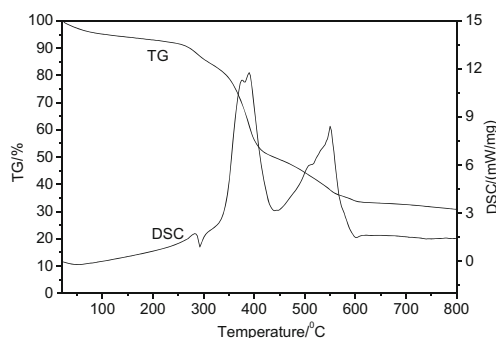
The thermogravimetric analysis of [EuL^a(NO$_3$)$_2$](NO$_3$)·H$_2$O were studied in the range of 20–800 °C. There is a little mass loss (observed value 2.24 %) from 20 to 150 °C, assigned to the desorption of one crystal water molecular [12] (calculated value 2.05 %). A endothermic peak appears at 292.4 °C, assigned to the loss of the outside one molecule nitrate, the weight loss percentage 7.15 % is close to the calculated value 7.05 %. Meanwhile, the mass loss between 376 and 390 °C is 58.13 %, and this value is consistent with the calculated value 50.39 % of organic ligand decomposition. The last weight loss percentage is 14.30 % at 554 °C, corresponding to the loss of internally two molecules nitrate (calculated value 14.11 %). A further increase in temperture from 560 °C leads to the decomposition of the ligand L^a. Up to 800 °C, when the complex is completely decomposed, the remaining solid is Eu$_2$O$_3$, and the mass loss percentage 18.18 % is close to the calculated value 17.40 %. The thermal analysis results show that the target complex has high thermal stability.

Fluorescence Properties Analysis

The fluorescence spectra data of [EuL$^{a–d}$(NO$_3$)$_2$](NO$_3$)·H$_2$O are listed in Table 5. Since the observed fluorescence spectra of all the Eu^{3+} complexes are very similar, only the fluorescence spectrum of [EuL^c(NO$_3$)$_2$](NO$_3$)·H$_2$O is selected for illustration, and its excitation and emission spectra are shown in Figs. 6 and 7.

It can be seen from Fig. 6 that the complex [EuL^c(NO$_3$)$_2$](NO$_3$)·H$_2$O exhibits a broad band in the 320–380 nm region (λ_{max}=364 nm), so the wavelength at 364 nm

Fig. 5 The TG-DSC curve of [EuL^a(NO$_3$)$_2$](NO$_3$)·H$_2$O

Table 5 The fluorescence spectra data of the europium complexes

Complex	λ_{ex}/nm	$^5D_0 \rightarrow ^7F_1$		$^5D_0 \rightarrow ^7F_2$	
		λ_{em} /nm	I/a.u.	λ_{em} /nm	I/a.u.
[EuL^a(NO$_3$)$_2$](NO$_3$)·H$_2$O	364	595	365.7	620	1,458
[EuL^b(NO$_3$)$_2$](NO$_3$)·H$_2$O	364	594	106.4	620.5	514.6
[EuL^c(NO$_3$)$_2$](NO$_3$)·H$_2$O	364	594.5	910.2	620	3,410
[EuL^d(NO$_3$)$_2$](NO$_3$)·H$_2$O	364	595	726.5	621	2,624
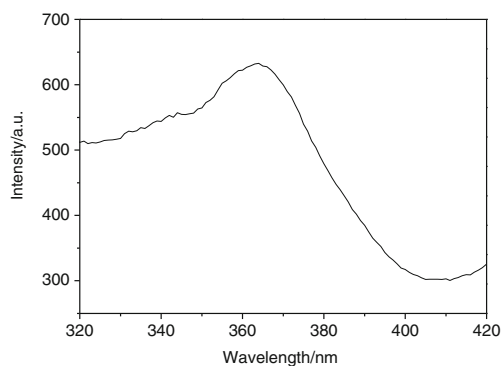
Fig. 6 The excitation spectrum of $[EuL^c(NO_3)_2](NO_3) \cdot H_2O$

was used to measure the fluorescence intensities of all the complexes. The emission spectra of the complex $[EuL^c(NO_3)_2](NO_3) \cdot H_2O$ exhibits one sharp characteristic emission peak at 620 nm corresponding to the $^5D_0 \rightarrow {}^7F_2$ transition, whereas the $^5D_0 \rightarrow {}^7F_1$ transition at 594.5 nm is observed. Additionally, the strongest emission intensity of $^5D_0 \rightarrow {}^7F_2$ transition (electric dipole) is 3410, while that of the $^5D_0 \rightarrow {}^7F_1$ transition (magnetic dipole) is 910.2, and the former is about 3.75 times stronger than the latter. The sharp emission peak at 620 nm indicates that the complex has good monochromaticity and the energy transfered from the excited triplet state of the ligand to the vibrational state of the europium ion is efficient [13].

Table 5 shows that the fluorescence intensities of the $^5D_0 \rightarrow {}^7F_2$ transition and the $^5D_0 \rightarrow {}^7F_1$ transition of the complex $[EuL^b(NO_3)_2](NO_3) \cdot H_2O$ are 514.6 and 106.4, respectively, which are lower than that of other complexes. This is due to the ligand L^b having an electron-withdrawing group (−Cl). The fluorescence intensities of the $^5D_0 \rightarrow {}^7F_2$ transition and the $^5D_0 \rightarrow {}^7F_1$ transition of the complexes $[EuL^c(NO_3)_2](NO_3) \cdot H_2O$ and $[EuL^d(NO_3)_2](NO_3) \cdot H_2O$ are 3410 and 910.6, 2624 and 726.5, respectively, which are stronger than that of the complex $[EuL^a(NO_3)_2](NO_3) \cdot H_2O$. This is attributed to the ligands L^c and L^d having electron-donating groups (−CH_3 and −OCH_3, respectively). The above results show that the electron-withdrawing group on the ligand can decrease the fluorescence intensity of the complex,
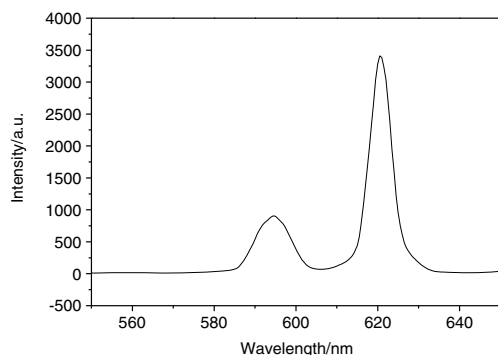
Fig. 7 The emission spectrum of $[EuL^c(NO_3)_2](NO_3) \cdot H_2O$

and this is due to (i) the electron-withdrawing group can reduce electron density of the phenyl ring in the complex, and (ii) the introduction of the electron-withdrawing group can easily result in fluorescence quenching [14]. On the contrary, the electron-donating group on the ligand results in an increase in the fluorescence intensity of the complex, which is due to the electron-donating group can donate electrons to the aromatic ring and enlarge the π-conjugated system of the ligand.

Whereas, the fluorescence intensity of the complex $[EuL^c(NO_3)_2](NO_3) \cdot H_2O$ is the strongest in all the Eu^{3+} complexes. The theory of antenna effect [15] can explain the result and the theory is described as following. The free Eu^{3+} ions have a low absorbance in rather narrow bands, and the direct excitation yields only a weak fluorescence. If a stable complex is formed with a suitable organic ligand which can transfer its excitation energy to Eu^{3+} ions, the fluorescence intensity of Eu^{3+} ions can be strengthened. Based on this theory, the fluorescence intensity of the Eu^{3+} complex is related to the efficiency of the intramolecular energy transfered from the triplet state of the ligand to the vibrational state of the Eu^{3+} ions, which depends on the energy gap (Eg) between the two states. Methyl group on L^c can donate electrons to the aromatic ring and enlarge the π-conjugated system, resulting in the triplet state of L^c corresponding with the lowest excited state of Eu^{3+} ions and the efficiency of the intramolecular energy transfered from the triplet state of L^c to the vibrational state of the Eu^{3+} ions is higher than other ligands. At the same time, all complexes show characteristic lines for the sensitization of Eu^{3+} ions, which shows that the energy can be absorbed and transferred to central Eu^{3+} ions effectively [16]. The above results further highlight that the nature of the substituted group has a significant effect on the fluorescence intensity of the Eu^{3+} complex.

Fluorescence Quantum Yields Analysis

The fluorescence quantum yields (Φ_{fx}) of the Eu^{3+} complexes were determined using a sulfuric acid solution (0.1 mol/L) of quinine sulfate (1.0 μg/mL) with a known quantum yield ($\Phi_{fstd} = 0.55$) as standard reference at room temperature because of the similarly between its absorption and fluorescent spectra with those of the target complexes. The fluorescence quantum yields (Φ_{fx}) are calculated by a comparative method [17] using the following equation.

$$\Phi_{fX} = \frac{n_X^2}{n_{std}^2} \cdot \frac{F_X}{F_{std}} \cdot \frac{A_{std}}{A_X} \cdot \Phi_{fstd}$$

Where n_x (1.48) and n_{std} (1.34) are the refractive indices of solvents used for the sample and standard. F_x and F_{std} are the areas under the fluorescence curves of the sample and

Table 6 The fluoresence quantum yields of the europium complexes

Complexes	λ_{ex}/nm	I/a.u.	F_X	Fluorescent quantum yield(Φ_{fx})
[EuL^a(NO$_3$)$_2$](NO$_3$)·H$_2$O	324	1,247	65304.094	0.372
[EuL^b(NO$_3$)$_2$](NO$_3$)·H$_2$O	326	915	48471.198	0.297
[EuL^c(NO$_3$)$_2$](NO$_3$)·H$_2$O	321	1,654	83896.377	0.467
[EuL^d(NO$_3$)$_2$](NO$_3$)·H$_2$O	320	1,568	78550.520	0.415

standard. A_x and A_{std} are the absorbances of the sample and standard at the excitation wavelength, respectively. Both the sample and standard are excited at the same relevant wavelength, so that the A_{std} is equal to A_x. The fluorescence quantum yields data of all the Eu^{3+} complexes are summarized in Table 6.

As shown in Table 6, the quantum yields of the complexes [EuL^c(NO$_3$)$_2$](NO$_3$)·H$_2$O and [EuL^d(NO$_3$)$_2$](NO$_3$)·H$_2$O are 0.467 and 0.415, respectively, and the complex [EuL^c(NO$_3$)$_2$](NO$_3$)·H$_2$O exhibits the highest quantum yield, resulting from the larger donor character of the methyl group and the larger π-conjugated system of the phenyl. The quantum yield of the complex [EuL^a(NO$_3$)$_2$](NO$_3$)·H$_2$O is 0.372. By contrast, [EuL^b(NO$_3$)$_2$](NO$_3$)·H$_2$O shows the lowest quantum yield (0.297). This is because the n→π* transition of chlorine substituent belongs to forbidden transition, and the excited state molecules are seldom obtained [18]. The results reveal that the electron-donating group can increase the fluorescence quantum yield of Eu^{3+} complex and electron-withdrawing group can decrease the fluorescence quantum yield of Eu^{3+} complex.

Electrochemical Properties Analysis

The electrochemical properties of the Eu^{3+} complexes were investigated by means of a cyclic voltammetric technique in DMSO solution. The highest occupied molecular orbital (HOMO) energy levels and lowest unoccupied molecular orbital (LUMO) energy levels of the Eu^{3+} complexes were estimated according to the electrochemical performance and the UV absorption spectra [19]. The HOMO and LUMO data for the Eu^{3+} complexes are obtained using equation $E_{HOMO}=4.74+eE_{OX}$, $E_{LUMO}=-Eg+E_{HOMO}$, $Eg=1,240/\lambda_{onset}$(eV) (λ_{onset} is the largest UV absorption spectra peak starting value) [20]. All cyclic voltammetrics are depicted in Fig. 8 and their electrochemical data are listed in Table 7.

As shown in Table 7, the oxidation potential and HOMO energy level of [EuL^d(NO$_3$)$_2$](NO$_3$)·H$_2$O are higher than the values of [EuL^a(NO$_3$)$_2$](NO$_3$)·H$_2$O, while the oxidation potential and HOMO energy level of the complexes [EuL^{b,c}(NO$_3$)$_2$](NO$_3$)·H$_2$O are slightly declined. The results may be due to the various substituent types of the ligands. The electron-donating group is benefit to improving the oxidation potential and HOMO energy level, and the introduction of electron-withdrawing group will reduce oxidation potential

and HOMO energy level. In all the Eu^{3+} complexes, methoxyl-substituted Eu^{3+} complex shows the highest oxidation potential and HOMO energy level. The energy gap of the Eu^{3+} complexes is range from 4.715 to 4.751 eV, which indicated that the electron-donating groups and electron-withdrawing groups have no apparent effect on the energy gap. Moreover, the introduction of electron-donating group can increase the HOMO energy level, LUMO energy level and the oxidation potential of the Eu^{3+} complex and the introduction of electron-withdrawing groups tend to decrease HOMO energy level, LUMO energy level and the oxidation potential of the Eu^{3+} complex. The frontier orbital theory [21] may provide an explanation for the above phenomena; the HOMO energy level possesses the priority to provide electrons. For electron donor compounds, the oxidation process corresponds to the process of losing electrons in HOMO energy level.

Conclusions

Four novel salicyladehyde salicyhydrazone derivatives and their corresponding europium complexes were synthesized and characterized. The resluts of elemental analysis showed the formulas of the complexes were [EuL^{a-d}(NO$_3$)$_2$](NO$_3$)·H$_2$O. The results of IR spectra showed the nitrogen atom of C=N group, the oxygen atoms of N-C=O groups and two nitrate groups coordinated to the Eu^{3+} ions. The thermal study indicated that the Eu^{3+} complexes were thermally stable. The fluoresence properties of the Eu^{3+} complexes were also investigated. The results showed the fluorescence intensity of the
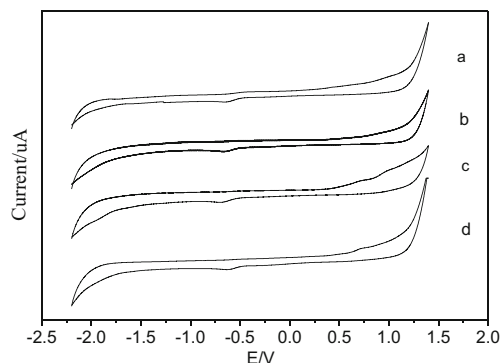
Fig. 8 The CV curves of [EuL^{a-d}(NO$_3$)$_2$](NO$_3$)·H$_2$O

Table 7 The E_{HOMO}, E_{LUMO} and Eg of the europium complexes

Complex	λ_{onset} /nm	Eox/v	E_{HOMO} /ev	Eg/ev	E_{LUMO}/ev
[EuL^a(NO$_3$)$_2$](NO$_3$)·H$_2$O	261	0.637	5.377	4.751	0.626
[EuL^b(NO$_3$)$_2$](NO$_3$)·H$_2$O	261	0.627	5.367	4.751	0.616
[EuL^c(NO$_3$)$_2$](NO$_3$)·H$_2$O	263	0.615	5.355	4.715	0.640
[EuL^d(NO$_3$)$_2$](NO$_3$)·H$_2$O	263	0.653	5.393	4.715	0.678

complex substituted by methyl (−CH$_3$) was the strongest among all the Eu^{3+} complexes. The exploration of the electrochemical properties of the Eu^{3+} complexes showed that the introduction of electron-donating groups methyl and methoxyl (−CH$_3$ and −OCH$_3$) could increase the oxidation potential and the highest HOMO energy level of the Eu^{3+} complexes; however, the result of introduction of electron-withdrawing group was just opposite. These results demonstrate that the title Eu^{3+} complexes possess good application prospects and theoretical research value.

References

1. Ieda LVR, Paulo CSF, Claudio CRN et al (2011) Synthesis and study of the photophysical properties of a new Eu^{3+} complex with 3-hydroxypicolinamide. J Fluoresc 21:1575–1583
2. Liang B, Liu XR, Zhang PH (2010) Synthesis and properties of o-carboxybenzaldehyde salicyloylhydrazone. Chin J Org Chem 30:1580–1583
3. Guo DC, Wu PL, Tan H et al (2011) Synthesis and luminescence properties of novel 4-(N-carbazole methyl) benzoyl hydrazone schiff bases. J Lumin 131:1272–1276
4. Li WX, Chai WJ, Sun XJ et al (2010) Synthesis and luminescence properties of two novel lanthanide(III) perchlorate complexes with bis(benzoylmethyl) sulfoxide and benzoic acid. J Fluoresc 20:873–880
5. Han FB, Teng QQ, Zhang Y et al (2011) Influence of schiff base and lanthanide metals on the synthesis, stability, and reactivity of monoamido lanthanide complexes bearing two schiff bases. J Inorg Chem 50:2634–2643
6. Ren QX, Zhai YC, Sun YY et al (2010) Synthesis and spectral analysis of coordination compounds of glucosamine with Eu(NO$_3$)$_3$ and Tb(NO$_3$)$_3$. Chem World 10:586–589
7. He SY, Chen YL, Yang R et al (2003) Synthesis, spectrum study and biological activity of salicylaldehyde salicylhydrazone complexes with rare earth. Chin J Org Chem 23:1387–1392
8. Guo DC, He W, Yu XQ et al (2013) Synthesis and luminescence properties of N-carbazole acetyl hydrazones schiff-bases. Lumin 28:280–286
9. Wang BD, Yang ZY, Zhang DW et al (2006) Synthesis, structure, infrared and fluorescence spectra of new rare earth complexes with 6-hydroxy chromone-3-carbaldehyde benzoyl hydrazone. Spectrochim Acta A 63:13–19
10. Sun LN, Qiu YN, Liu T (2013) Near infrared and visible luminescence from xerogels covalently grafted with lanthanide [Sm^{3+}, Yb^{3+}, Nd^{3+}, Er^{3+}, Pr^{3+}, Ho^{3+}] β-diketonate derivatives using visible light excitation. Appl Mater Inter 5:9585–9593
11. Kong K, Zhang HX, Ma RJ (2013) Synthesis, characterization and enhanced luminescence of terbium complexes with 2-pyrazinecarboxylic acid and butanedioic acid by inert-fluorescent lanthanide ions. J Rare Earths 31:2–6
12. Tang RR, Zhang W, Luo YM et al (2009) Synthesis, fluorescence properties of Eu(III) complexes with novel carbazole functionalized β-diketone ligand. J Rare Earths 27:362–367
13. Li WX, Li YJ, Chai WJ et al (2012) Syntheses and fluorescence properties of two novel lanthanide(III) perchlorate complexes with bis(benzylsulfinyl)methane. J Fluoresc 22:651–658
14. Zhang XP, Wen XP, Hu S et al (2010) Luminescence properties of Eu(III) complex/polyvinylpyrrolidone electrospun composite nanofibers. J Phys Chem 114:3898–3903
15. Chang YW, Yang JJ (2006) Synthesis, characterization and luminescence properties of rare earth complexes with bis(pyridinyl-amide). Chin J Rare Earth 24:146–151
16. Masahisa O, Mikio H, Tatsuo W et al (2009) Intra-complex energy transfer of europium(III) complexes containing anthracene and phenanthrene moieties. J Phys Chem A 113:10895–10902
17. Li LD, Zhang M (1988) Comparative method for determining fluorescence quantum yield. Anal Chem 16:732–734
18. Soustek P, Michl M, Almonasy N et al (2008) The synthesis and fluorescence of N-substituted 1- and 2-aminopyrenes. Dyes Pigments 78:139–147
19. Pablo MR, Carmen C, Angel LA et al (2013) Charge transport and sensitized 1.5 μm electroluminescence properties of full solution-processed NIR-OLED based on novel Er(III) fluorinated β-diketonate ternary complex. J Phys Chem C 117:10020–10030
20. Ding BD, Zhang JM, Zhu WQ et al (2002) Fast and convenient determination of HOMO energy level of organic electroluminescent material using electrochemistry method. Chem Res Appl 14:712–714
21. Tamar S, Jochen A, Niranjan G et al (2012) Curvature and frontier orbital energies in density functional theory. J Phys Chem Lett 3:3740–3744